

# Improved Methods for Processing Optical Mapping Signals From Human Left Ventricular Tissues at Baseline and Following Adrenergic Stimulation

María Pérez-Zabalza<sup>1</sup>, Emiliano R Diez<sup>2,3</sup>, Julia Rhyins<sup>4</sup>, Kostantinos A Mountris<sup>1</sup>, José M Vallejo-Gil<sup>5</sup>, Pedro C Fresneda-Roldán<sup>5</sup>, Javier Fañanás-Mastral<sup>5</sup>, Marta Matamala-Adell<sup>5</sup>, Fernando Sorribas-Berjón<sup>5</sup>, Manuel Vázquez-Sancho<sup>5</sup>, Carlos Ballester-Cuenca<sup>5</sup>, Margarita Segovia-Roldán<sup>1</sup>, Aida Oliván-Viguera<sup>1</sup>, Esther Pueyo<sup>1,6</sup>

<sup>1</sup> Aragón Institute of Engineering Research, IIS Aragón, University of Zaragoza, Zaragoza, Spain

<sup>2</sup> Institute of Experimental Medicine and Biology of Cuyo (IMBECU), CONICET, Mendoza, Argentina

<sup>3</sup> Department of Physiology, School of Medicine, National University of Cuyo, Mendoza, Argentina

<sup>4</sup> Northeastern University Bioengineering, Boston, USA

<sup>5</sup> Department of Cardiovascular Surgery, University Hospital Miguel Servet, Zaragoza, Spain

<sup>6</sup> CIBER in Bioengineering, Biomaterials and Nanomedicine (CIBER-BBN), Madrid, Spain

## Abstract

*Optical mapping (OM) allows ex vivo measurement of electrophysiological signals at high spatio-temporal resolution, but the signal-to-noise ratio is commonly low. A variety of software options have been proposed to extract relevant information from OM recordings, being ElectroMap the most advanced tool currently available. In this study, improved methods are presented for processing OM signals of cardiac transmembrane voltage. A software called OMap is developed that incorporates novel techniques into ElectroMap for improved baseline drift removal, spatio-temporal filtering and characterization of action potential duration (APD) maps. In synthetically generated signals contaminated with baseline wander, white noise and the combination of both, the errors in APD maps between noisy and clean signals are remarkably lower for OMap than for ElectroMap, particularly for high noise levels. In OM signals recorded from human ventricular tissue specimens, OMap allows to clearly characterize the APD shortening effect induced by  $\beta$ -adrenergic stimulation, whereas ElectroMap renders highly overlapped APD distributions for baseline and  $\beta$ -adrenergic stimulation. In conclusion, improved methods are proposed and tested to characterize human ventricular electrophysiology from noisy OM recordings.*

## 1. Introduction

Optical mapping (OM) is a fluorescence imaging technique used to study cardiac electrophysiological signals.

OM uses fluorescent dyes to ex vivo measure transmembrane voltage or intracellular calcium at high spatio-temporal resolution, without direct tissue contact. OM recordings commonly have low signal-to-noise ratios due to the small light intensities and short exposure times when high speed cameras are used at frames rates above 500 Hz. The effects of noise are particularly remarkable when mapping small tissue preparations, where noise levels can be comparable to the amplitude of the signal [1].

A number of approaches have been proposed in the literature to process OM recordings so that meaningful information on cardiac electrical activity can be extracted from them. One of the latest approaches that has been recently made available as open-source software is ElectroMap [2], which provides additional functionalities to those offered by other non-commercial (Rhythm [3]) and commercial (BV\_Ana - SciMedia, Optiq - Cairn Research) software options. In those software as well as in other published methods for OM signal processing, strategies have been proposed to deal with noise and robustly analyze cardiac activation or repolarization properties. On the one hand, methods based on strong spatial and temporal filtering have been presented to extract relevant information even if sometimes at the expense of morphological signal distortion [4]. On the other hand, stacking methods based on overlapping images from equidistant time intervals have been suggested to reduce noise even if this can be at the expense of losing information on beat-to-beat variability [1]. Both types of methods are incorporated in ElectroMap.

In this study, improved methods for processing OM signals are presented and applied onto recordings ob-

tained from human ventricular tissue specimens. The proposed methods depart from those available in the open-source software ElectroMap and incorporate new processing functionalities. On the one hand, novel techniques for baseline drift removal, based on high-pass filtering or on cubic spline and linear interpolation, have been added. Also, additional options for adaptive spatio-temporal filtering and for selection of regions with high enough SNR have been included. We evaluate the performance of our optimized software, in the following called OMap, and compare it with that of ElectroMap using a set of synthetically generated signals. We subsequently apply OMap and Electromap onto optically mapped slices of human ventricular tissue specimens, before and after administration of the  $\beta$ -adrenergic agonist isoproterenol.

## 2. Materials and Methods

### 2.1. Experimental data

Human left ventricular papillary muscle specimens resected during valve replacement were collected at Miguel Servet University Hospital. Patients gave full informed consent for the study, which conforms to the principles outlined in the Declaration of Helsinki and was approved by the local Ethics Committee (Ref. PI17/0023). The collected specimens from five patients were immediately submerged in cold, pre-oxygenated Tyrode solution: NaCl 140 mM, KCl 6 mM, MgCl<sub>2</sub> 1 mM, CaCl<sub>2</sub> 1.8 mM, 2,3-Butanedione monoxime (BDM) 30 mM, HEPES 10 mM. 350  $\mu$ m-thick slices were vibratome sectioned in ice-cold (4°C) preoxygenated 30 mM BDM-Tyrode's solution. The slices were loaded with 10  $\mu$ M blebbistatin (30 min), 7.5  $\mu$ M Rhod-2 (30 min) and 7.5  $\mu$ M RH237 (15 min) to measure transmembrane voltage and intracellular calcium concentration. Next, the slices were placed in a dish with clean Tyrode solution for a 30-to-60-minute washing step, following which OM recordings were acquired while pacing at 1 Hz.  $\beta$ -adrenergic stimulation responsiveness was evaluated by application of isoproterenol hydrochloride (100 nM, Sigma Aldrich) slowly washed into the bath solution. OM signals were normalized in amplitude to the interval [0 1].

### 2.2. Synthetic data

Synthetic transmembrane voltage signals were generated by simulating electrical propagation in a  $3 \times 3$  cm<sup>2</sup> human left ventricular tissue. The O'Hara-Virág-Varró-Rudy human ventricular action potential (AP) model [5] was used to simulate endocardial, midmyocardial and epicardial cardiomyocytes in a spatial configuration as reported experimentally [6]. The tissue was paced at 1 Hz from the left side. A longitudinal diffusion coefficient of

0.0013 cm<sup>2</sup>/ms and a transversal-to-longitudinal conductivity ratio of 0.25 were used. Simulations were performed using the in-house software ELECTRA implementing the Meshfree Mixed Collocation Method and the Finite Element Method, the latter used in this study for the solution of the monodomain model [7].

Different types of noise were added onto the clean synthetic signals (see Figure 1) to emulate the OM recordings acquired experimentally, as in previous studies [4]. Noise associated with baseline drift,  $b(n)$ , was generated as a linear combination of sinusoidal waves with uniformly distributed random phases  $\theta_k \in [0; 2\pi)$ , uniformly distributed random amplitudes  $a_k \in [0; 1]$  and frequency  $f = 0.06$  Hz:

$$b(n) = C \cdot \sum_{k=0}^K a_k \cos(2\pi k f n + \Theta_k). \quad (1)$$

(Quasi-)random noise was generated as white noise signals with normally distributed random amplitudes. Baseline drift noise was equally added for all elements of the simulated tissue, whereas the level of white noise was gradually increased from the most internal to the most external parts of the tissue in three degrees. Synthetic signals were normalized in amplitude to the interval [0 1].

According to the type of noise added to the signal, three groups were distinguished, each comprising five different noise levels: Drift ( $K = 8$  and  $C = [0.25, 0.5, 1, 1.25, 1.5]$ ); White noise (with the following noise powers in W for different areas within the tissue from the most internal (A1) to the most external (A3):  $A1 = [0.05, 0.1, 0.25, 0.5, 0.75]$ ,  $A2 = [1.5, 3.5, 5.5, 7.5, 9.5]$ ,  $A3 = [11.5, 12.5, 13.5, 14.5, 16.5]$ ); Drift + White noise ( $C = 0.5$ ,  $K = 8$  and the same white noise levels as in the White noise group).

### 2.3. Data processing

OM and synthetic signals were filtered in time and space and baseline drift was corrected. The processed signals were subsequently stacked to improve SNR and a second baseline correction was applied to remove potential remaining drifts in the stacked signals. The details of each of these processing steps are described next.

OMap incorporated the following processing options into the currently available ElectroMap software. First, a recently published adaptive spatio-temporal Gaussian filter that allows automatic selection of parameter values was added [4]. In particular, the value for a temporal filtering parameter  $\sigma_t$  was determined from the input data, which was used for the definition of a 1D Gaussian filter with a filter mask length of  $6\sigma_t + 1$ . This is in contrast to ElectroMap, which used a third order Savitzky-Golay temporal filter. For both OMap and ElectroMap, a spatial  $4 \times 4$ -pixel Gaussian ( $\sigma_s = 1.5$ ) filter was used.

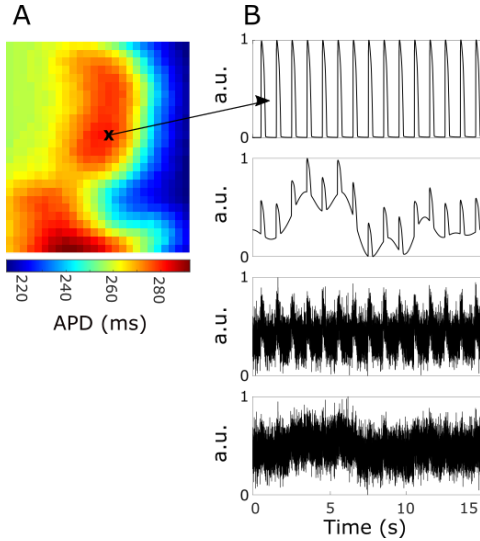


Figure 1: **A.** APD map for simulated electrical activity in a human ventricular tissue. **B.** From top to bottom: noiseless synthetic APs for the pixel marked with 'x'; APs with added baseline drift; APs with added white noise; APs with added baseline drift and white noise.

Second, additional techniques for baseline drift removal based on high-pass filtering or on cubic spline and linear interpolation, on top of already available techniques based on other polynomial fittings, were added. In this study, baseline drift in the spatio-temporally filtered signals was removed by high-pass filtering with a cut-off frequency of 0.4 Hz. ElectroMap, however, used a 11th-order polynomial to fit the baseline wander.

Third, for both OMap and ElectroMap, stacking was performed by averaging the signals corresponding to equidistant intervals of 1000 ms. AP duration (APD) was computed at 80% repolarization.

Fourth, a method for SNR calculation and optimal display of APD and activation maps was introduced into OMap. Maps were initially calculated for the whole set of pixels. A SNR value was calculated for each of them as the ratio of the AP amplitude divided by the root-mean-square of voltage during the diastolic interval [8]. A threshold on SNR was set and APD and activation maps were presented only for pixels with SNR above it.

## 2.4. Performance evaluation

OMap's performance was compared with that of ElectroMap when applied onto synthetically generated signals. APD was computed for each pixel in the mapped tissue for both the clean signals as well as for the noisy signals after the addition of baseline drift, white noise or both. The absolute error ( $e_{APD}$ ) between the APD values for the clean

signals and each of the noisy versions were calculated.

## 3. Results and Discussion

### 3.1. Study on synthetic signals

Figure 2A shows APD maps for an example of noiseless synthetically generated signals (central panel) and APD maps for noisy versions calculated with ElectroMap (left panel) and OMap (right panel). The gray area corresponds to pixels with SNR below the established threshold. As can be observed, the APD map computed with OMap reliably matches the clean APD map, whereas the APD map computed with ElectroMap shows remarkably less agreement.

Figure 2B shows the statistical distributions of absolute errors for signals with different levels of added baseline drift (top), white noise (middle) and both (bottom). It can be observed from the top panel that the median value of the absolute errors is similar for ElectroMap and OMap. In the case of adding white noise, the middle panel shows that ElectroMap has both higher median and interquartile ranges (IQR) than OMap. The bottom panel corresponding to cases with the two types of noises shows that OMap is able to better deal with them, even if not providing measurements for some of the pixels deemed as excessively noisy to render reliable measurements (shown in gray in Figure 2A). Median and IQR of absolute errors were notably lower for OMap, particularly for high levels of noise.

### 3.2. Study on optical mapping signals

Figure 3 illustrates the results for APD maps obtained with ElectroMap and OMap for an optically mapped human ventricular tissue slice before (panel A) and after (panel B) isoproterenol administration. The effect of APD shortening by isoproterenol can be clearly observed from the maps calculated with OMap while it is not evident from those calculated with ElectroMap. Panel C in Figure 3 shows APD histograms for both software. The OMap histograms allow separation of the statistical distributions corresponding to baseline and  $\beta$ -adrenergic stimulation, whereas ElectroMap histograms show more overlapped distributions. This performance was similarly observed for other slices of the same ventricular tissue specimen as well as for all other analyzed tissues.

## 4. Conclusions

Improved methods for processing OM signals have been proposed and tested. The new software, OMap, has been compared with the most updated software ElectroMap over a set of synthetically generated signals contaminated with noise. OMap outperformed ElectroMap in all cases, particularly under high noise levels. In tissue slices from human

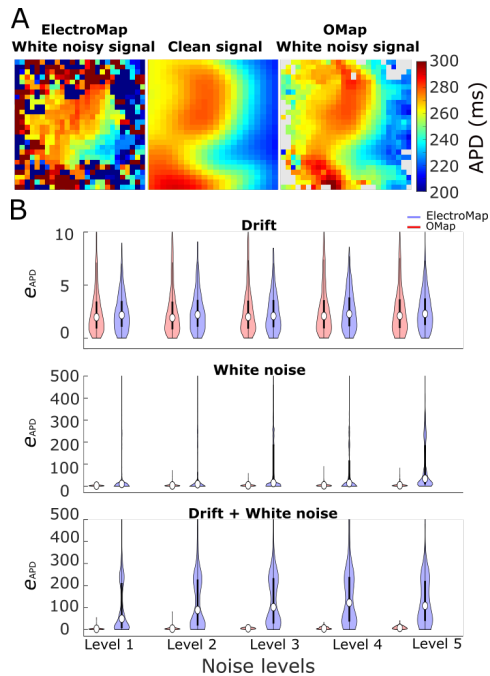


Figure 2: Results for synthetic signals. **A.** Central panel: APD map for a clean simulated tissue; Left and right panels: APD maps for noise-corrupted tissue as processed with ElectroMap and OMap. **B.** Violin plots showing the distribution of absolute errors for synthetic noisy signals.

ventricular specimens, OMap was able to reliably characterize APD maps and distinguish the APD shortening effect induced by  $\beta$ -adrenergic stimulation.

## Acknowledgements

This work was supported by projects ERC-StG 638284 (ERC), PID2019-105674RB-I00 (MICINN) and LMP124-18 and BSICoS T39-20R (Aragón Government cofunded by FEDER 2014-2020 "Building Europe from Aragon"). Computations were performed using ICTS NANBIOSIS (HPC Unit at University of Zaragoza).

## References

- [1] Uzelac I, Fenton FH. Robust framework for quantitative analysis of optical mapping signals without filtering. *CinC* 2015;461-464.
- [2] O'Shea C, Holmes A, Yu T, Winter J, Wells S, Correia J, Boukens B, Groot J, Chu G, Li X, Ng G, Kirchhof P, Fabritz L, Rajpoot K, Pavlovic D. Electromap: High-throughput open-source software for analysis and mapping of cardiac electrophysiology. *Sci Rep* 2019;9(1):1389.
- [3] Gloschat C, Aras K, Gupta S, Ndeye Rokhaya F, Zhang H, Syunyaev R, Pryamonosov R, Rogers J, Kay M, Efimov

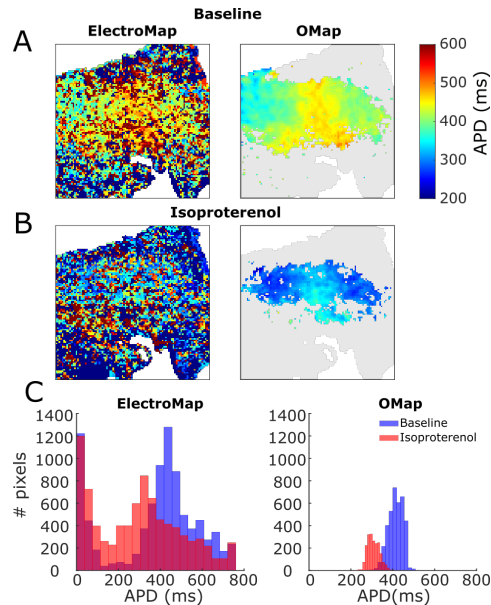


Figure 3: Results for optically mapped human left ventricular tissue. **A and B.** APD maps, before and after administration of isoproterenol, calculated with ElectroMap (left) and OMap (right). **C.** APD histograms, before (blue) and after (red) isoproterenol administration.

- I. Rhythm: An open source imaging toolkit for cardiac panoramic optical mapping. *Sci Rep* 2018;8(1):2921.
- [4] Pollnow S, Pilia N, Schwaderlapp G, Loewe A, Dössel O, Lenis G. An adaptive spatio-temporal Gaussian filter for processing cardiac optical mapping data. *Comput Biol Med* 2018;102:267-277.
- [5] O'Hara T, Virág L, Varro A, Rudy Y. Simulation of the undiseased human cardiac ventricular action potential: Model formulation and experimental validation. *PLoS Comput Biol* 2011;7(5):e1002061.
- [6] Glukhov A, Fedorov V, Lou Q, Ravikumar V, Kalish P, Schuessler R, Moazami N, Efimov I. Transmural dispersion of repolarization in failing and non failing human ventricle. *Circ Res* 2010;106(5):981-91.
- [7] Mountris KA, Sanchez C, Pueyo E. A novel paradigm for in silico simulation of cardiac electrophysiology through the Mixed Collocation Meshless Petrov-Galerkin method. *CinC* 2019;1-4.
- [8] Mironov S, Vetter F, Pertsov A. Fluorescence imaging of cardiac propagation: Spectral properties and filtering of optical action potentials. *Am J Physiol Heart Circ Physiol* 2006; 291(1):H327-35.

Address for correspondence:

María Pérez-Zabalza  
BSICoS group, University of Zaragoza, Campus Río Ebro, D-5.01.1B, Mariano Esquillor, s/n, 50018, Zaragoza, Spain  
mariapzabalza@unizar.es